Criterion for determining clustering versus reentrant melting behavior for bounded interaction potentials

C. N. Likos,[1,*] A. Lang,[1,2] M. Watzlawek,[1,†] and H. Löwen[1]
[1]*Institut für Theoretische Physik II, Heinrich-Heine-Universität Düsseldorf, Universitätsstraße 1, D-40225 Düsseldorf, Germany*
[2]*Institut für Theoretische Physik and CMS, Technische Universität Wien, Wiedner Hauptstraße 8-10, A-1040 Wien, Austria*
(Received 29 March 2000; revised manuscript received 16 October 2000; published 27 February 2001)

We examine in full generality the phase behavior of systems whose constituent particles interact by means of potentials that do not diverge at the origin, are free of attractive parts, and decay fast enough to zero as the interparticle separation r goes to infinity. By employing a mean field-density functional theory which is shown to become exact at high temperatures and/or densities, we establish a criterion that determines whether a given system will freeze at all temperatures or it will display reentrant melting and an upper freezing temperature.

DOI: 10.1103/PhysRevE.63.031206 PACS number(s): 61.20.Gy, 64.70.−p

I. INTRODUCTION

The phase behavior of systems whose constituent particles interact by means of pair potentials diverging at the origin is a problem that has been extensively studied in the last few decades. The whole range of inverse power-law pair potentials have been examined, ranging from hard spheres (HS's) to the one-component plasma (OCP) and it has been established that excluded volume effects are mainly responsible for bringing about the freezing transition. The crystal structure in which a liquid freezes is subsequently determined by the steepness of the repulsion, with hard repulsions favoring a face centered cubic (fcc) lattice and soft ones a body centered cubic (bcc) lattice [1]. Power-law diverging potentials result into freezing at arbitrarily high temperatures. However, the divergence of the potential alone is not enough to cause such a phenomenon, as demonstrated recently by Watzlawek *et al.* [2] who employed a logarithmically divergent pair potential, suitable to describe effective interactions between star polymers in good solvents. It was shown that the strength (prefactor) of the logarithmic potential, determined by the number of arms f of the stars, is crucial in determining whether the system freezes or remains fluid at all densities. As a consequence, the phase diagram of star polymers was predicted to display reentrant melting and a critical freezing value $f_c=34$ of arms, such that for $f<f_c$ the system remains always fluid [2].

Another interesting class of interactions are those which do not diverge at the origin, i.e., they are bounded. Such potentials arise naturally as effective interactions between the centers of mass of soft, flexible macromolecules such as polymer chains [3], dendrimers [4], polyelectrolytes, etc. Indeed, the centers of mass of two macromolecules can coincide without violation of the excluded volume conditions, hence bringing about a bounded interaction. Moreover, the same mechanisms that exist for tuning the usual, diverging interactions between colloidal particles can be applied in order to tune the bounded interactions: the solvent quality, temperature, chain length, salt concentration, etc., will all affect the effective potential. Thus, it appears to be useful to consider such potentials in some generality in order to be able to draw conclusions about the expected phase behavior of systems interacting by means of these.

Two model systems in this category have already been studied in some detail. One is the penetrable spheres model (PSM) [5,6], in which the pair potential is a positive constant ε for distances $r<\sigma$ and vanishes otherwise. The other is the Gaussian core model (GCM), introduced in the mid 1970's by Stillinger [7]. In the GCM, the pair potential $v(r)$ has the form $v(r)=\varepsilon \exp[-(r/\sigma)^2]$, with ε being an energy and σ a length scale. It has been shown that the GCM models very accurately the effective interactions between the centers of mass of linear polymer chains [3,8–14].

The PSM was studied by means of cell-model calculations and computer simulations [6], liquid-state integral equation theories [15], and density-functional theory [16]; the fluid structure of the PSM has been further studied recently by Rosenfeld *et al.* by using ideas based on the universality of the bridge functional [17]. It was found that no reentrant melting takes place because the solid always lowers its free energy by allowing for multiply occupied crystal sites, a mechanism that is called clustering [6]. The clustering mechanism stabilizes therefore the solid at all temperatures. Hence, the topology of the phase diagram of the PSM is similar to that of power-law diverging potentials, when details about the clustering structure of the solids are disregarded. On the other hand, the GCM has been studied even more extensively by means of molecular dynamics simulations [18,19], high-temperature expansions [20], and the discovery of exact duality relations in the crystalline state [21]. Recently, a full statistical-mechanical study of the GCM was performed and it was established that the topology of the phase diagram of the GCM resembles that of star polymers. Freezing and reentrant melting accompanied by an upper freezing temperature were quantitatively calculated [22]. The question that arises, therefore, is the following. Given a nonattractive and bounded pair potential which satisfies the following requirements guaranteeing stability and the existence of the thermodynamic limit [23]: (i) it is bounded, (ii) it is positive definite, (iii) it decays fast enough to zero at large

*Email address: likos@thphy.uni-duesseldorf.de
†Present address: Bayer AG, Central Research Division, D-51368 Leverkusen, Germany

 ©2001 The American Physical Society

separations, so that it is integrable and its Fourier transform exists, and (iv) it is free of attractive parts; to which topology belongs the phase diagram of the system? In this paper, we present an exact criterion which gives an answer to this question and show representative results for model systems that confirm its validity. The rest of the paper is organized as follows: in Sec. II we present the physical arguments supporting the mean-field theory of the models and in Sec. III we discuss the existence of a spinodal instability in this theory and its implications on the phase behavior. We present a systematic comparison between theory and simulation in Sec. IV and we draw the generic phase diagrams of such systems in Sec. V. Finally, in Sec. VI we summarize and conclude.

II. THE MODEL AND THE MEAN-FIELD LIMIT

We will work with a general interaction $v(r)=\varepsilon\phi(r/\sigma)$ satisfying the requirements put forward above. Here, ε and σ are an energy and a length, respectively, and $\phi(x)$ is some dimensionless function. The latter does not have to be analytic, i.e., discontinuities in the potential or its derivatives are allowed. Without loss of generality, we assume $\phi(0)=1$. Let us call $\hat{\phi}(Q)=\sigma^{-3}\tilde{\phi}(Q)$ the dimensionless Fourier transform (FT) of the interaction. For more concreteness (and for the purposes of demonstration) we introduce in addition the family of bounded potentials $v_\xi(r)$ depending on a tunable parameter ξ,

$$v_\xi(r)=\varepsilon\frac{1+e^{-\sigma/\xi}}{1+e^{(r-\sigma)/\xi}}, \tag{1}$$

where ξ is a ''smoothing parameter'' having dimensions of length. The case $\xi=0$ recovers the PSM whereas as ξ grows the interaction becomes smoother. Due to its resemblance to the Fermi-Dirac distribution, we call this family the Fermi distribution model (FDM). The additional factor $1+e^{-\sigma/\xi}$ in the numerator of the RHS of Eq. (1) ensures that the potential varies from ε at $r=0$ to zero at $r\to\infty$, for all ξ.

We introduce dimensionless measures of temperature and density as

$$t=\frac{k_BT}{\varepsilon}=(\beta\varepsilon)^{-1}, \tag{2}$$

$$\eta=\frac{\pi}{6}\rho\sigma^3=\frac{\pi}{6}\overline{\rho}, \tag{3}$$

where k_B is Boltzmann's constant and $\rho=N/V$ is the density of a system of N particles in the volume V. We will refer to η as the ''packing fraction'' of the system.

The key idea for examining the high temperature and/or high density limit of such model systems is the following. We consider in general a spatially modulated density profile $\rho(\mathbf{r})$ which does not vary too rapidly on the scale σ set by the interaction. At high densities, $\rho\sigma^3\gg1$, the average interparticle distance $a\equiv\rho^{-1/3}$ becomes vanishingly small, and it holds $a\ll\sigma$, i.e., the potential is extremely long range. Every particle is simultaneously interacting with an enormous number of neighboring molecules and in the absence of short-range excluded volume interactions the excess free energy of the system [24] can be approximated by a simple mean-field term, equal to the internal energy of the system:

$$F_{\mathrm{ex}}[\rho(\mathbf{r})]\cong\frac{1}{2}\int\int d\mathbf{r}d\mathbf{r}'v(|\mathbf{r}-\mathbf{r}'|)\rho(\mathbf{r})\rho(\mathbf{r}'), \tag{4}$$

with the approximation becoming more accurate with increasing density. Then, Eq. (4) immediately implies that in this limit the direct correlation function $c(r)$ of the system, defined as [24]

$$c(|\mathbf{r}-\mathbf{r}'|;\rho)=-\lim_{\rho(\mathbf{r})\to\rho}\frac{\delta^2\beta F_{\mathrm{ex}}[\rho(\mathbf{r})]}{\delta\rho(\mathbf{r})\,\delta\rho(\mathbf{r}')}, \tag{5}$$

becomes independent of the density and is simply proportional to the interaction, namely,

$$c(r)=-\beta v(r). \tag{6}$$

Using the last equation, together with the Ornstein-Zernike relation [25], we readily obtain an analytic expression for the structure factor $S(Q)$ of the system as

$$S(Q)=\frac{1}{1+\overline{\rho}t^{-1}\hat{\phi}(Q)}. \tag{7}$$

This mean-field approximation (MFA) has been put forward and examined in detail in the context of the Gaussian core model independently by Lang *et al.* [22] and by Louis *et al.* [26]. The model is particularly relevant from the physics point of view, due to its connection to the theory of effective interactions between polymer chains [3,14]. Here, we establish the validity of the MFA at high densities for bounded, positive-definite interactions in general and we examine its implications for the global phase behavior of such systems.

Bounded and positive-definite interactions have been studied in the late 1970's by Grewe and Klein [27,28]. The authors considered a slightly different model than the one considered here, namely, a Kac potential of the form

$$v(r)=\gamma^d\psi(\gamma r), \tag{8}$$

where d is the dimension of the space and $\gamma\geqslant0$ is a parameter controlling the range and strength of the potential. Moreover, $\psi(x)$ is a non-negative, bounded and integrable function

$$0\leqslant\psi(x)\leqslant A<\infty,\quad C=\int d^d\mathbf{x}\psi(x)<\infty. \tag{9}$$

Grewe and Klein were able to show rigorously that at the limit $\gamma\to0$, the direct correlation function of a system interacting by means of the potential (8) is given by Eq. (6) above. The connection with the case we are discussing here is straightforward: as there are no hard cores in the system or a lattice constant to impose a length scale, the only relevant length is set by the density and is equal to $\rho^{-1/3}$ in our model and by the parameter γ^{-1} in model (8). In this respect, the

limit $\gamma \to 0$ in the Kac model of Grewe and Klein is equivalent to the limit $\rho \to \infty$ considered here. However, in the Kac model the strength of the interaction goes to zero simultaneously with the increase in its range. Moreover, the validity of the mean-field expression at large but finite densities and at low temperatures has not been tested in detail.

III. SPINODAL INSTABILITY AND FREEZING

We employ the MFA as a physically motivated working hypothesis for now and, by direct comparison with simulation results, we will show later that it is indeed valid. Within the framework of this theory, an exact criterion can be formulated, concerning the stability of the liquid phase at high temperatures and densities. The function $\phi(x)$ was assumed to be decaying monotonically from unity at $x=0$ to zero at $x \to \infty$. For the function $\hat{\phi}(Q)$, there are two possibilities: (i) It has a monotonic decay from the value $\hat{\phi}(Q=0) = \sigma^{-3} \int d\mathbf{x} \phi(x) > 0$ to the value $\hat{\phi}(Q) = 0$ at $Q \to \infty$. We call such potentials Q^+ potentials. Obviously, the Gaussian interaction belongs to this class. (ii) It has oscillatory behavior at large Q, with the implication that it is a nonmonotonic function of Q, attaining necessarily negative values for certain ranges of the wave number. We call such potentials $Q^{\pm}$ potentials. Long-range oscillations in Q space imply that $\phi(x)$ changes more rapidly from unity at $r=0$ to zero at $r \to \infty$ in the $Q^{\pm}$ class than in the Q^+ one. Moreover, let us call Q_* the value of Q at which $\hat{\phi}(Q)$ attains its minimum, negative value.

If we are dealing with a $Q^{\pm}$ potential Eq. (7) implies that $S(Q)$ has a maximum at precisely the wave vector Q_* where $\hat{\phi}(Q)$ attains its negative minimum $-|\hat{\phi}(Q_*)|$ and this maximum becomes a singularity at the ''spinodal line'' $\overline{\rho} t^{-1} |\hat{\phi}(Q_*)| = 1$, signaling the so-called Kirkwood instability of the system [28–31]. The theory has a divergence, implying that the underlying assumption of a uniform liquid is not valid and the system must reach a crystalline state. Indeed, on the basis of the fluctuation-dissipation theorem, $S(Q)$ can be interpreted as a response function of the density to an infinitesimal external modulating field at wave number Q [25] and a diverging value of this response function clearly signals an instability. If the Fourier transform of $\phi(x)$ has negative Fourier components, then an increase in temperature can be compensated by an increase in density in the denominator of Eq. (7), so that $S(Q_*)$ will have a divergence at all t. We thus conclude that $Q^{\pm}$ systems freeze at all temperatures.

If we are dealing with a Q^+ potential [$\hat{\phi}(Q)$ monotonic], then Eq. (7) implies that $S(Q)$ is also a monotonic function of Q at high densities [22]. For such potentials, one can always find a temperature high enough, so that the assumptions of Eq. (4) hold and then Eq. (7) forces the conclusion that freezing of the system is impossible at such temperatures. This does not imply, of course, that such systems do not freeze at all; one simply has to go to a low enough temperature and density, so that the mean-field assumption does not hold and the interaction is much larger that the thermal energy. Then, the system will display a hard-sphere type of freezing, to be discussed more explicitly below. An upper freezing temperature t_u must exist for Q^+ potentials, implying that such systems must remelt at $t < t_u$ upon increase of the density. Hence, we reach the conclusion that Q^+ systems display an upper freezing temperature and reentrant melting. The criterion says nothing about the crystal structure of the solid, however, which always depends on the details of the interaction as well as the density [22,32].

For potentials is in the Q^+ class, the mean-field arguments presented above hold not only at high temperatures but also at low ones, provided that the requirement $\rho\sigma^3 \gg 1$ is satisfied, because these are molten at high densities for all nonzero temperatures. The validity of the mean-field theory for Q^+-type systems, even at very low temperatures, was confirmed recently by direct comparison with simulation results for the particular case of the Gaussian potential [22]. If the potential is in the $Q^{\pm}$ class, the mean field approximation holds provided that the system is not already frozen, as we will confirm shortly. Moreover, both kinds of systems display an unusual kind of ''high density ideal gas'' limit. Indeed, taking the expression (7) for $S(Q)$ and using the relation $S(Q) = 1 + \overline{\rho} \hat{h}(Q)$ [25], where $\hat{h}(Q)$ is the dimensionless Fourier transform of the pair correlation function $h(r)$ of the uniform fluid, we obtain

$$\hat{h}(Q) = -\frac{t^{-1}\hat{\phi}(Q)}{1 + \overline{\rho} t^{-1} \hat{\phi}(Q)}. \tag{10}$$

At low Q's, where $\hat{\phi}(Q)$ is of order unity, the term proportional to the density in the denominator dominates in the limit of high densities and $\hat{h}(Q)$ scales as $-1/\overline{\rho} \to 0$. At high Q's, the Fourier transform $\hat{\phi}(Q)$ in the numerator is itself small, with the result that $\hat{h}(Q)$, and hence also the correlation function $h(r)$, is approaching zero. This, in turn, means that the radial distribution function $g(r) = h(r) + 1$ is very close to unity in this limit and deprived of any significant structure for all values of r and it only has some small structure at small r, which is in fact more pronounced for $Q^{\pm}$ potentials than for Q^+ ones. In this limit, the hypernetted chain (HNC) closure becomes exact, as the exact relation $g(r) = \exp[\beta v(r) + h(r) - c(r) - B(r)]$, combined with the limits $g(r) \to 1$, $h(r) \to 0$, and $c(r) \to -\beta v(r)$ forces the bridge function $B(r)$ to vanish. Moreover, Eqs. (7) and (10) reveal that the systems obey a scaling law, namely that the functions $S(Q)$ and $th(r)$ do not depend on $\overline{\rho}$ and t separately but only on the ratio $\overline{\rho}/t$.

Systems in the $Q^{\pm}$ class freeze before the spinodal is reached. In order to make quantitative predictions, we invoke the empirical Hansen-Verlet freezing criterion [33,34], which states that a system crystallizes when $S(Q)$ at its main peak attains, approximately, the value $S(Q_*) = S_m \cong 3$. Although this criterion was originally put forward for hard, atomic interactions (HS, Lennard-Jones, etc.), recent detailed analyses have demonstrated that it holds for the freezing and the remelting transitions of ultrasoft particles such as star polymers [2,35] and even for the nondiverging Gaussian interac-

tion [22]. Hence, we assume that it is valid for the general class of systems we consider here and combining it with Eq. (7), we obtain the equation of the freezing line $t_f(\eta)$ as

$$t_f(\eta)=\frac{6|\hat{\phi}(Q_*)|}{\pi(1-S_m^{-1})}\,\eta\cong 2.864|\hat{\phi}(Q_*)|\,\eta. \qquad (11)$$

The value $|\hat{\phi}(Q_*)|$ determines the slope of the freezing line at the high (t,η) part of the phase diagram.

IV. COMPARISON WITH SIMULATIONS

We now wish to put these arguments in a strong test, using the concrete family of the FDM, given by Eq. (1). First of all, we have calculated the Fourier transform of the potential $v_\xi(r)$ of Eq. (1) numerically, establishing that members of the FDM with $\xi<\xi_c$ belong to the $Q^{\pm}$ class and members with $\xi>\xi_c=0.49697$ to the Q^{+} one. The GCM is also a member of the latter class that we will discuss in what follows.

A. Systems displaying clustering

As examples of systems displaying clustering transitions, we have taken the extreme (and by now well-studied case) case $\xi=0$ (the PSM) as well as the case $\xi=0.1$ of the Fermi distribution model of Eq. (1). We have performed standard Monte Carlo (MC) *NVT* simulations for a large number of values for the temperature and density. We begin with the PSM for which the analytical expression (7) takes the form

$$S(Q)=\left[1+24\eta t^{-1}\left(\frac{\sin(Q\sigma)-(Q\sigma)\cos(Q\sigma)}{(Q\sigma)^3}\right)\right]^{-1}. \qquad (12)$$

The high-temperature–high-density freezing line of Eq. (11) takes for this choice of ξ the form $t_f(\eta)=1.033\eta$. To test the analytical expression of Eq. (12), we move along the ''diagonal'' $t=\eta$, a combination that lies almost on the Hansen-Verlet estimate for the location of the freezing line. In Fig. 1 we show the comparison of the analytical results with those obtained from the MC simulations for $S(Q)$ and we also demonstrate that the MC curves for the quantity $t(h(r))$ all collapse onto a single line, amply demonstrating the validity of the mean-field approximation for the PSM. In order to further investigate the validity of the MFA, we have performed MC simulations in a variety of thermodynamic points and we present a selection of the obtained results. We present a selection of these in Figs. 2 and 3 and discuss them below.

In Fig. 2(a) we show a comparison between the MC and MFA results for the radial distribution function $g(r)$ along the ''diagonal'' $t=\eta$. It can be seen that the agreement between the two is already very good at $t=\eta=4.0$ and thereafter it improves markedly with increasing temperature and density. The results obtained from the present theory are of the same quality as those obtained by Fernaud *et al.* [15], who used the sophisticated zero-separation (ZSEP) closure to investigate the liquid structure of the system. This closure involves three self-consistency parameters, determined in such a way that the virial-compressibility, Gibbs-Duhem and zero-separation consistency conditions are fulfilled. At the same time, the present results are of the same quality as the recently obtained results of Rosenfeld *et al.* [17], based on ideas of the universality of the bridge functional.

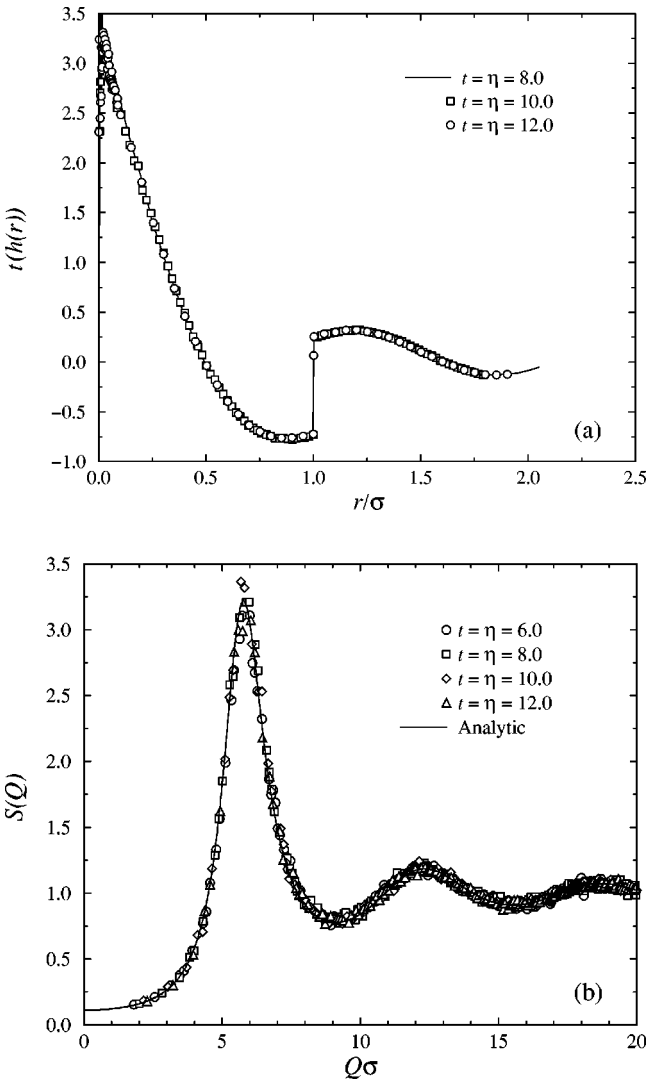

FIG. 1. (a) The product $t(h(r))$ for a FDM with $\xi=0$ PSM, along the diagonal $t=\eta$ at high packing fractions, as obtained from MC simulations. The results close to $r=0$ are noisy due to poor statistics there. All results collapse onto a single curve. (b) The corresponding structure factors $S(Q)$, shown together with the analytical result of Eq. (12).

In Fig. 2(b) we perform the same comparison but now at fixed temperature $t=5.0$ and increasing packing fraction η. As can be seen, at this temperature, the MFA, which was originally formulated as a high-density approximation, proves to perform extremely well even at intermediate packings, $\eta=0.5$, for instance. This is a direct consequence of the boundedness of the interaction combined with a temperature $t\gg\varepsilon$. Indeed, for small densities, the direct correlation function tends to the Mayer function, $c(r)\cong\exp[-\beta v(r)]-1$ [25]. If we are dealing with a bounded interaction at high

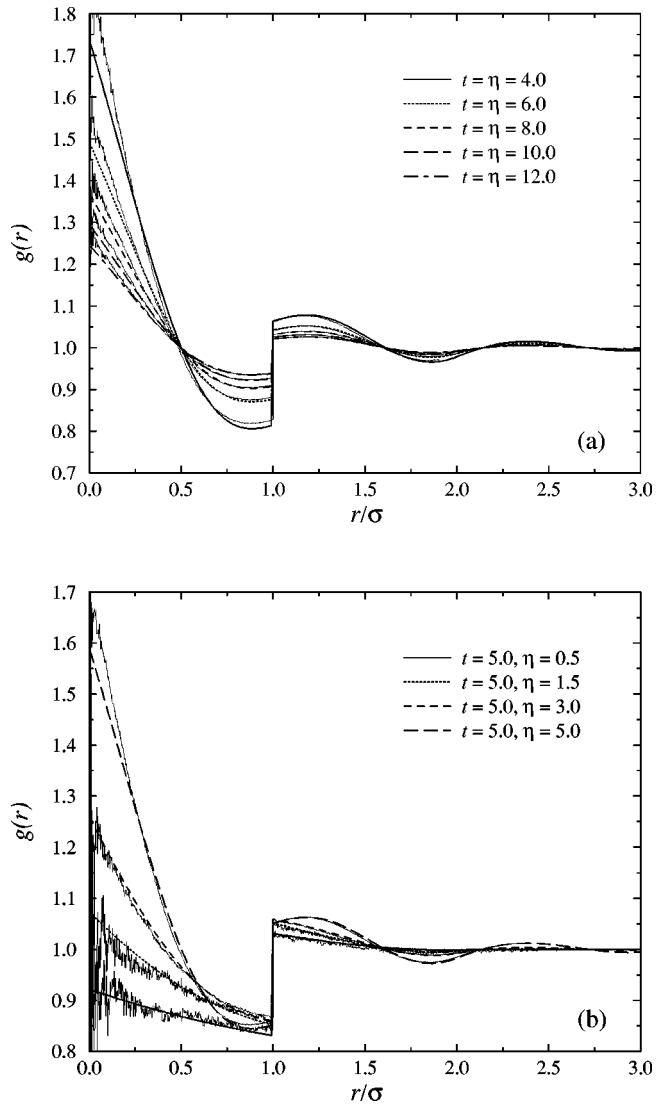

FIG. 2. (a) The function $g(r)$ of the PSM for selected points along the ''diagonal'' $t=\eta$ as obtained from theory (thick lines) and simulation (thin lines). (b) Same but now for fixed temperature $t=5$ and increasing packing fraction η.

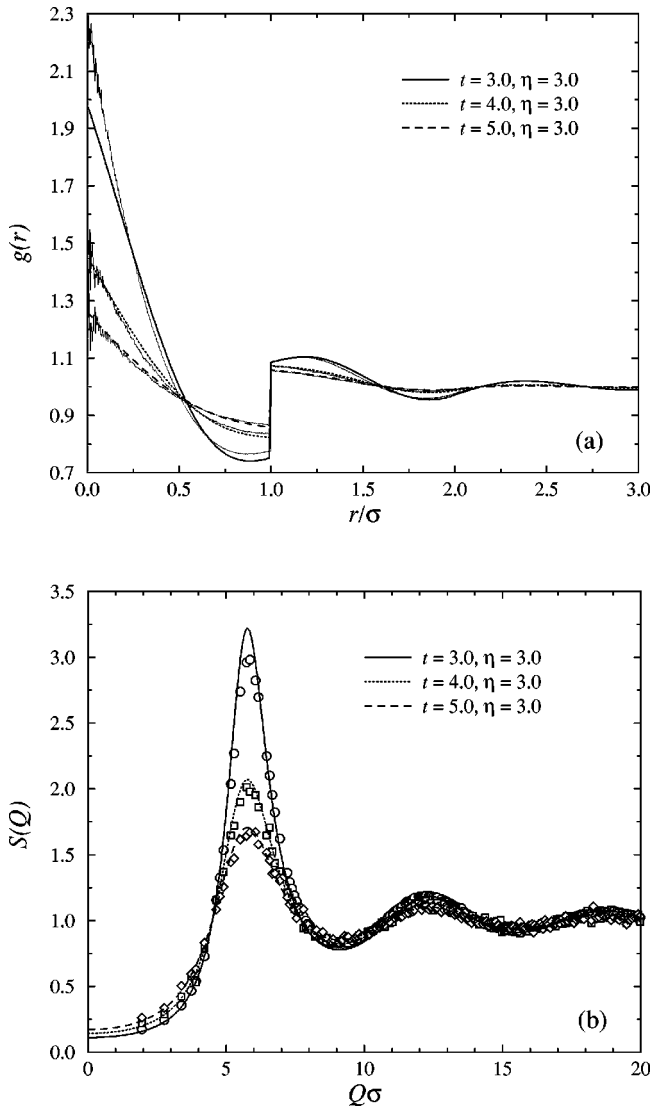

FIG. 3. (a) Same as Fig. 2(b) but now for fixed $\eta=3.0$ and increasing temperature. (b) The structure factors at the thermodynamic points of (a), comparison between theory (lines) and simulation (points).

temperature, we can linearize the exponential, obtaining $c(r)\cong-\beta v(r)$ at low densities, which matches with the MFA expression, Eq. (6), at high densities, thus leading to the conclusion that the MFA is an excellent approximation at *all densities*. For unbounded interactions the linearization of the exponential is evidently impossible.

In Fig. 3 we present a comparison between MC and MFA at fixed packing fraction $\eta=3.0$ and increasing temperature. As can be clearly seen, the validity of the MFA improves with increasing temperature. For bounded interactions, an increasing temperature implies a ''washing-out'' of the correlation effects caused by the (increasingly weak) interaction effects and a tendency of the system towards the particular ''high-density ideal gas'' limit characterized by the tendency of the function $g(r)$ towards unity. However, it is an interesting peculiarity of these systems that unlike the usual ideal gas, the limit $g(r)\rightarrow 1$ [or, equivalently, $h(r)\rightarrow 0$] does not imply a corresponding limit $S(Q)\rightarrow 1$. Though the Fourier transform of $h(r)$,$\hat{h}(Q)$, tends to zero as ρ^{-1}, this is compensated by the large density ρ, so that the structure factor $S(Q)=1+\rho\hat{h}(Q)$ displays the signature of strong ordering through the pronounced peaks seen in Figs. 1(b) and 3(b).

Further, we performed MC simulations at selected points deeply inside the region $t<t_f(\eta)$, finding that the obtained structure factors displayed Bragg peaks and hence confirming the prediction that the system is frozen there. Putting all our results together, we draw in Fig. 4 a semiquantitative phase diagram of the PSM, accompanied by an assessment of the validity of the MFA at selected thermodynamic points. The MFA appears to be an excellent approximation at all densities above the temperature $t=3.0$. Hence, we take as an estimate for the freezing line above $t=3.0$ the MFA-Hansen-Verlet line $t_f=1.033\eta\cong\eta$; for lower temperatures, we simply connect the point $(\eta,t)=(3.0,3.0)$ with the point $(\eta,t)=(0.5,0)$, which obtains from the consideration that at

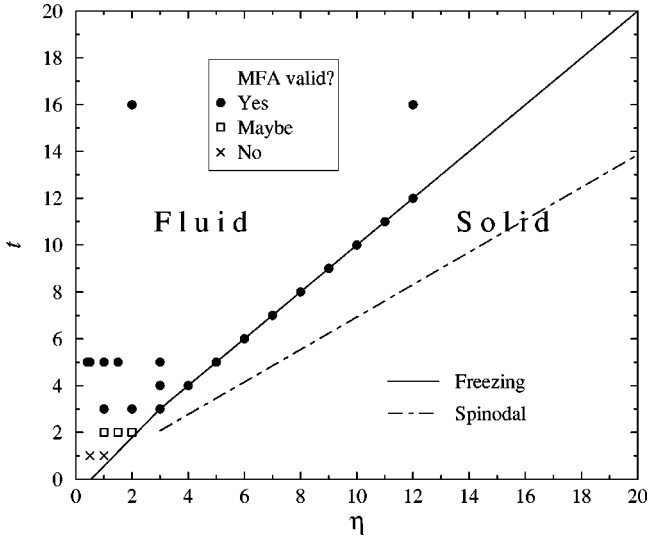

FIG. 4. The phase diagram of the PSM, along with the points where the mean field theory brings excellent agreement with simulation (filled circles), fairly good agreement (empty squares), and no good agreement (crosses). These symbols should help delineate the domain of validity of the mean-field theory.

$t=0$ the PSM reduces to the hard sphere system which is known to freeze at a fluid density $\eta_{\mathrm{HS}}\cong 0.5$. The monotonic shape of the freezing curve for low temperatures arises from detailed considerations there, which can be found in Ref. [6].

Next we present in Fig. 5(a) comparison for the FDM with $\xi=0.1$. For this choice of ξ, the Hansen-Verlet-based freezing line takes the form $t_f=0.712\eta$. The selected points lie in the fluid region and the comparison indicates once more the excellent accuracy of the MFA both for $g(r)$ and for $S(Q)$. The radial distribution function $g(r)$ of this model is deprived of the jump at $r=\sigma$ seen in the PSM; the latter is caused by the discontinuity of the PSM potential there. However, a similarity between the $g(r)$'s of the $\xi=0$ and $\xi=0.1$ models is that they both attain their maximum values at full overlaps between the particles $r=0$ and thereafter they decay rapidly, featuring a depletion region around $r\approx\sigma$. This is a characteristic pointing to a strong clustering property in the fluid phase, a property thereafter inherited by the incipient thermodynamically stable crystal; the number of particles ''sitting on top of each other'' and thereby occupying the same crystal site scales linearly with density. In order to corroborate this claim, we can argue in two different ways, using the liquid as a reference point.

First, let us consider the number of particles N_c in the fluid phase whose centers are, on average, within a distance σ from a given particle. The number N_c is given by the formula

$$N_c=1+4\pi\rho\int_0^{\sigma} r^2 g(r)dr. \tag{13}$$

In Fig. 6 we show the function $4\pi r^2 g(r)$ within a particle diameter σ for a sequence of points along the freezing line of the PSM. As all these curves tend to a common

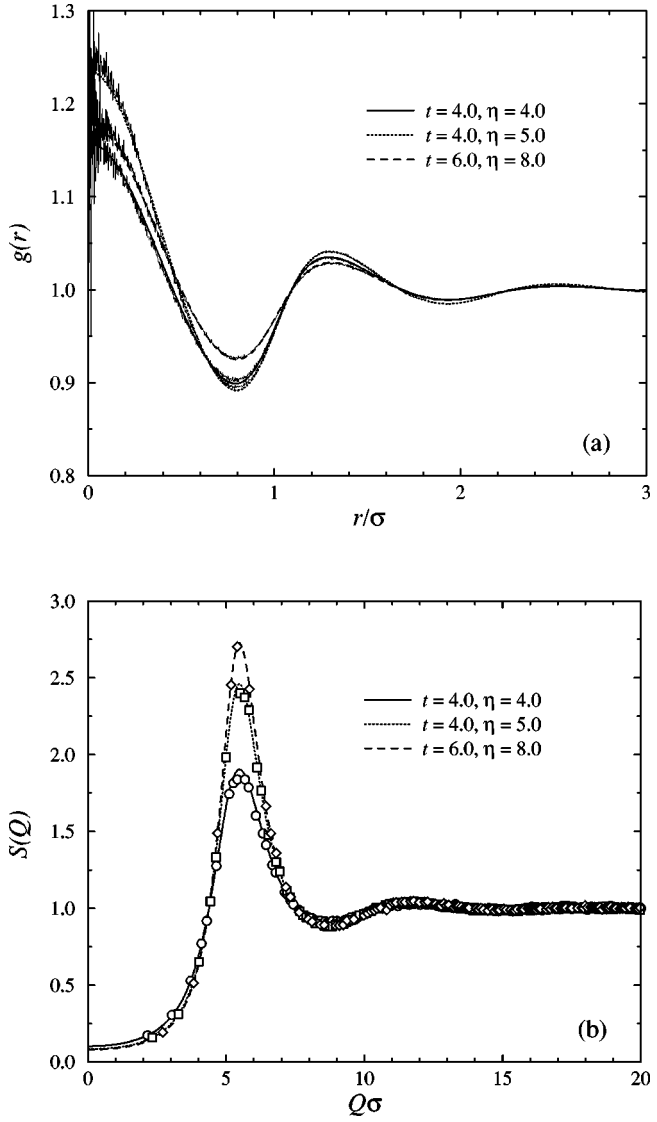

FIG. 5. (a) Comparison between theory (thick lines) and simulation (thin lines) results for $g(r)$ of a FDM system with $\xi=0.1$. (b) Comparison for the structure factors (lines: theory; points: simulation) for the same system at the thermodynamic points of (a).

limit with increasing density, the integral $4\pi\int_0^{\sigma} r^2 g(r)dr$ tends to a constant and hence $N_c\propto\rho$ at high densities, where the second term on the RHS of Eq. (13) dominates.

Second, we can use the wavevector Q_* at which the fluid structure factor has a maximum in order to estimate for the lattice constant a of the incipient crystal through the relation $a\propto Q_*^{-1}$. For the models at hand, this maximum is entirely determined by the pair potential; unlike in usual fluids featuring diverging interactions, for which Q_* scales as $\rho^{1/3}$, in our case Q_* knows nothing about the density. Thus, all post-freezing crystals have the same lattice constant, although their average density is a linear function of the temperature. This clearly shows that clustering must take place in the crystal: by allowing more and more particles to occupy the same lattice sites, a practically constant effective density of

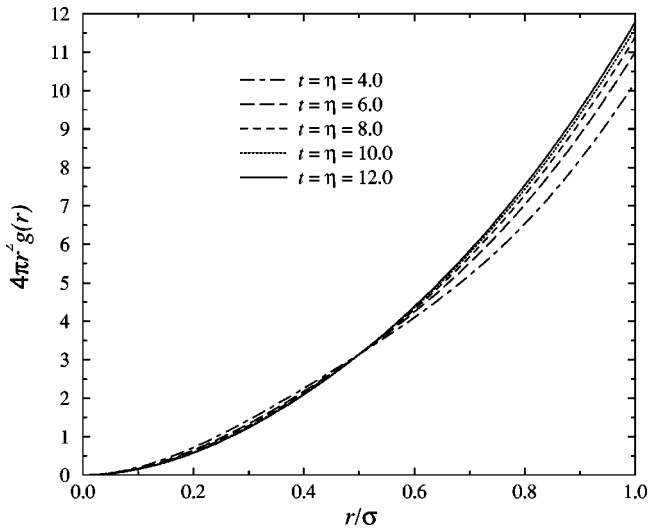

FIG. 6. The quantity $4\pi r^2 g(r)$ within the diameter σ of the PSM along the freezing line $t=\eta$. All the curves converge to a single one at high densities, indicating that the integral $4\pi\rho\int_0^\sigma r^2 g(r)dr$ scales linearly with density.

clusters is maintained in the crystal, thus leading to a density-independent lattice constant.

B. Systems displaying reentrant melting

We now turn our attention to the opposite case, namely pair potentials belonging to the Q^+ class. As an example within the FDM family, we have taken the model with parameter $\xi=0.6$ and performed a comparison between MC and MFA results. A characteristic example is shown in Fig. 7. As can be seen in Fig. 7(a), unlike the case of $Q^{\pm}$-class potentials, the radial distribution function is completely deprived of any structure, although the thermodynamic parameters are in the same regime as those presented in Figs. 2, 3, and 5. In fact, in the present case, $g(r)$ has a minimum at $r=0$, not a maximum. This complete lack of structure is reflected in the shape of $S(Q)$, shown in Fig. 7(b).

These characteristic features for the Q^+ class are not an artifact of the relatively high temperature chosen in the results of Fig. 7. They persist even at extremely low temperatures, provided the density is high enough. This has been amply demonstrated recently for the case of the Gaussian core model, another member of the Q^+ class [22]. In order to stress this point we present in Fig. 8 the $g(r)$ and $S(Q)$ of the GCM at $t=0.01$ and $\eta=6.0$. Though $g(r)$ displays some structure up to $r\approx 2\sigma$, the structure factor $S(Q)$ shows no signature of some kind of ordering [40]. At any arbitrarily small but finite temperature, a high enough density can be found for which the MFA is valid and then the assumption that a uniform phase exists leads consistently to a fluid which has ideal-gas behavior, i.e., vanishingly small correlations. These liquids are different from usual ideal gases in that, e.g., their pressure P and isothermal compressibility χ_T scale, respectively, as $P\sim\rho^2$ and $\chi_T\sim t\rho^{-2}$. Nevertheless, they are thermodynamically stable. Hence, for potentials in the Q^+ class, the equilibrium phase for sufficiently high densities at arbitrarily small but finite temperatures is the uniform fluid.

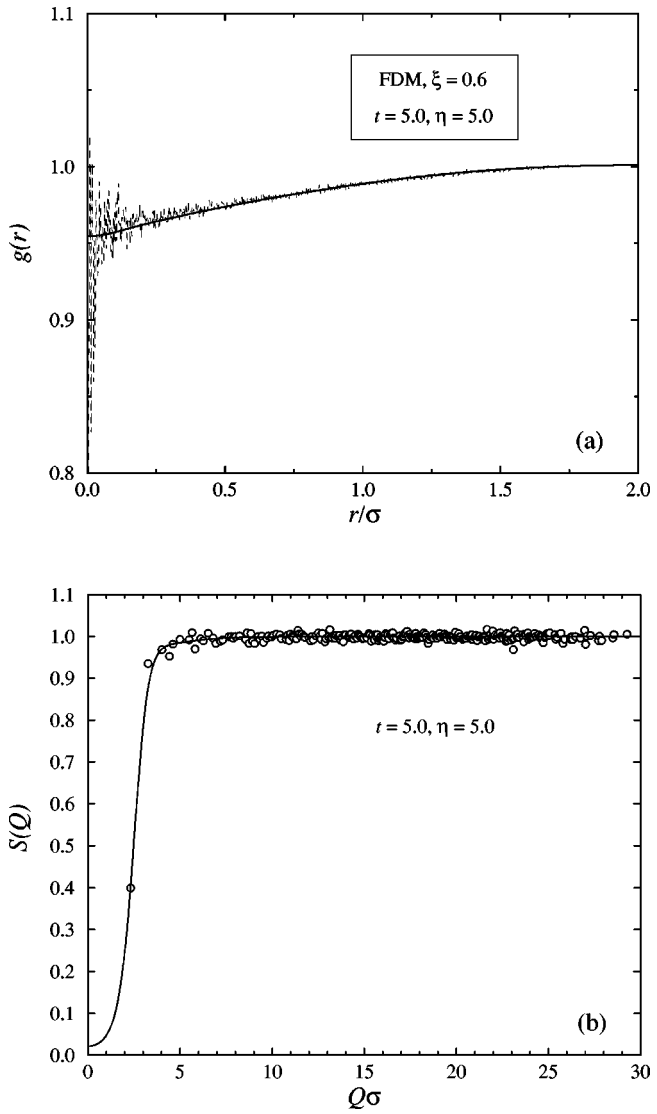

FIG. 7. (a) Comparison between theory (thick lines) and simulation (thin lines) results for $g(r)$ of a FDM system with $\xi=0.6$. (b) Comparison for the structure factor $S(Q)$ (lines: theory; points: simulation) for the same system at the thermodynamic point of (a).

V. GENERIC PHASE DIAGRAMS

We now turn to the opposite limit of the low-temperature–low-density part of the phase diagram. There, following the original ideas of Stillinger [7], a HS mapping can be performed, as follows. The Boltzmann factor $\exp[-\beta v(r)]$ of the potential varies monotonically from the value $\exp(-\beta\varepsilon)\cong 0$ (since $\beta\varepsilon\gg 1$ there) at $r=0$ to unity at $r\to\infty$ and has a close resemblance to that of a hard sphere system. We can thus define an effective hard sphere diameter $\sigma_{\rm HS}$ through the relation

$$\exp[-\beta v(\sigma_{\rm HS})]=1/2. \tag{14}$$

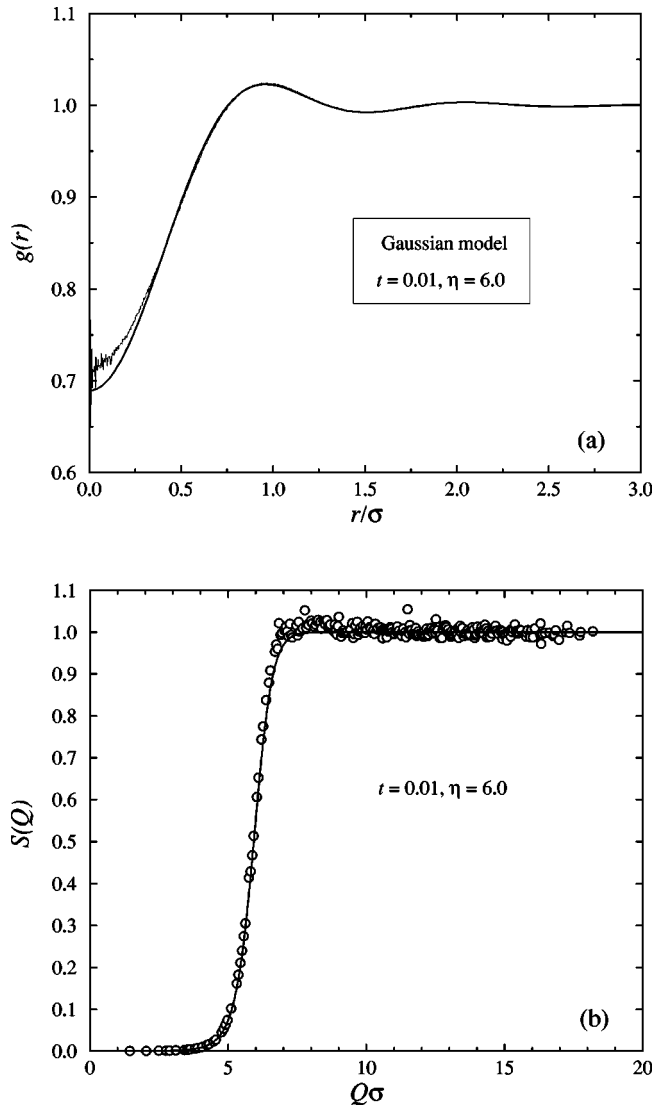

FIG. 8. Same as Fig. 7 but for the Gaussian core model.

Writing $v(r)=\varepsilon\phi(r/\sigma)$ and using the fact that $\phi(x)$ is a monotonic function in order to establish that the inverse function $\phi^{-1}(x)$ exists, we can rewrite Eq. (14) as

$$\sigma_{\mathrm{HS}}=\sigma\phi^{-1}(t\ln 2). \tag{15}$$

We now use the known fact hard spheres freeze at $\eta_{\mathrm{HS}}\cong 0.5$ together with Eq. (15) above in order to obtain the low temperature-low density freezing line of the system as

$$t_f(\eta)=\frac{1}{\ln 2}\,\phi[(2\eta)^{-1/3}]. \tag{16}$$

As the limit $\phi(x)\to 0$ is attained for $x\to\infty$ only, it follows that the low-temperature–low-density freezing line of the systems goes to $\eta=0$ at $t_f=0$. Eq. (16) is valid for all potentials we consider here; however, for Q^+ potentials, combining the HS-like freezing at low temperatures and densities with the fact that at high densities the fluid has to be stable,

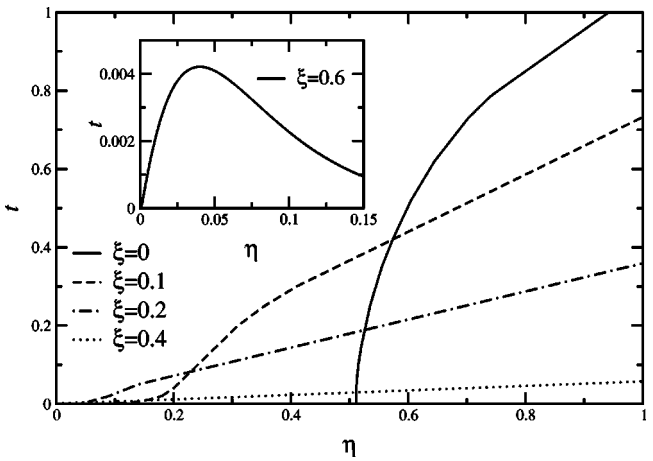

FIG. 9. The evolution of the phase diagram of $Q^{\pm}$ FDM's with ξ. To the right of the freezing lines the system is solid and to the left fluid. Inset: the phase diagram of a Q^+ FDM with $\xi>\xi_c$, obtained by solving the HNC and employing the Hansen-Verlet criterion. Below the bell-shaped curve the system is solid and above fluid.

derived in the preceding section, we can draw the conclusion that such systems must display reentrant melting and an upper freezing temperature.

We have now taken Eq. (16) for the low-t and low-η freezing line of the FDM and combined it with the analytic expression at the opposite limit, Eq. (11), in order to draw schematically the evolution of the phase diagram of the FDM as a function of ξ, for $\xi<\xi_c$. The results are shown in Fig. 9. With increasing ξ, the slopes of the high-t freezing lines decrease; at the limit $\xi\to 0$, corresponding to the PSM, the low-t freezing line approaches the horizontal axis vertically, as is dictated by the fact that the PSM becomes equivalent to the HS system there [6]. In the inset of Fig. 9, we show the phase diagram for a system with $\xi=0.6>\xi_c$, showing reentrant melting behavior. The evolution of the phase diagram from a clustering to a reentrant melting behavior can be easily visualized from this picture.

Finally, it is important to point out that Stillinger has proven that any system interacting by means of a potential which (i) is differentiable at least four times, (ii) vanishes strongly enough at infinity to be integrable, and (iii) is $+1$ at the origin, will inevitably lead to a reentrant melting phase diagram under the assumption that the competing crystal structures have single lattice site occupancy [7]. We can therefore now complete the statement and say that if a potential belongs to the Q^+ class, then it will freeze into crystals of single occupancy and then remelt upon increase of the density. But if it belongs to the $Q^{\pm}$ class, then it will freeze into a clustered solid at any temperature. Clustering appears therefore to be the crucial mechanism for crystal stabilization in these systems.

VI. SUMMARY AND CONCLUDING REMARKS

To summarize, we have established a criterion for the topology of the phase diagrams resulting from repulsive, bounded interactions, which is very simple in its formulation

and states that if the Fourier transform of the pair potential is positive definite, then the system shows reentrant melting but if not then it freezes at all temperatures, into clustered crystals with multiple occupied sites. We have also established that at temperatures exceeding the interaction strength the mean-field theory is reliable at all densities and its accuracy improves quickly with increasing temperature. We close with the remark that there is a certain similarity between the ideas put forward here and the considerations on freezing for systems featuring of diverging interactions at infinite spatial dimensions [36–39]. However, in the latter case, the direct correlation function is given by the Mayer function $f(r)=\exp[-\beta v(r)]-1$ of the interaction potential and not by $-\beta v(r)$ as in the case at hand.

ACKNOWLEDGMENTS

This work was supported by the Österreichische Forschungsfond under Project Nos. P11194-PHY and P13062-TPH. A.L. acknowledges financial support by the Deutsche Forschungsgemeinschaft within the SFB 237.

[1] G. A. McConnell, A. P. Gast, J. S. Huang, and S. D. Smith, Phys. Rev. Lett. **71**, 2102 (1993).
[2] M. Watzlawek, C. N. Likos, and H. Löwen, Phys. Rev. Lett. **82**, 5289 (1999).
[3] A. A. Louis, P. G. Bolhuis, J.-P. Hansen, and E. J. Meijer, Phys. Rev. Lett. **85**, 2522 (2000).
[4] C. N. Likos, M. Schmidt, H. Löwen, M. Ballauff, D. Pötschke, and P. Lindner, e-print cond-mat/0010235.
[5] C. Marquest and T. A. Witten, J. Phys. (Paris) **50**, 1267 (1989).
[6] C. N. Likos, M. Watzlawek, and H. Löwen, Phys. Rev. E **58**, 3135 (1998).
[7] F. H. Stillinger, J. Chem. Phys. **65**, 3968 (1976).
[8] O. F. Olaj and W. Lantschbauer, Ber. Bunsenges. Phys. Chem. **81**, 985 (1977).
[9] A. Y. Grosberg, P. G. Khalatur, and A. R. Khokhlov, Makromol. Chem., Rapid Commun. **3**, 709 (1982).
[10] L. Schäfer and A. Baumgärtner, J. Phys. (Paris) **47**, 1431 (1986).
[11] B. Krüger, L. Schäfer, and A. Baumgärtner, J. Phys. (Paris) **50**, 3191 (1989).
[12] J. Dautenhahn and C. K. Hall, Macromolecules **27**, 5933 (1994).
[13] A. A. Louis, R. Finken, and J.-P. Hansen, Europhys. Lett. **46**, 741 (1999).
[14] P. G. Bolhuis, A. A. Louis, J.-P. Hansen, and E. J. Meier, e-print cond-mat/0009093.
[15] M. J. Fernaud, E. Lomba, and L. L. Lee, J. Chem. Phys. **112**, 810 (2000).
[16] M. Schmidt, J. Phys.: Condens. Matter **11**, 10 163 (1999).
[17] Y. Rosenfeld, M. Schmidt, M. Watzlawek, and H. Löwen, Phys. Rev. E **62**, 5006 (2000).
[18] F. H. Stillinger and T. A. Weber, J. Chem. Phys. **68**, 3837 (1978).
[19] F. H. Stillinger and T. A. Weber, Phys. Rev. B **22**, 3790 (1980).
[20] F. H. Stillinger, J. Chem. Phys. **70**, 4067 (1979).
[21] F. H. Stillinger, Phys. Rev. B **20**, 299 (1979).
[22] A. Lang, C. N. Likos, M. Watzlawek, and H. Löwen, J. Phys.: Condens. Matter **24**, 5087 (2000).
[23] D. Ruelle, *Statistical Mechanics* (Benjamin, New York, 1969).
[24] R. Evans, Adv. Phys. **28**, 143 (1979).
[25] J.-P. Hansen and I. R. McDonald, *Theory of Simple Liquids*, 2nd ed. (Academic Press, London, 1986).
[26] A. A. Louis, P. G. Bolhuis, and J.-P. Hansen, Phys. Rev. E **62**, 7961 (2000).
[27] N. Grewe and W. Klein, J. Math. Phys. **64**, 1729 (1977).
[28] N. Grewe and W. Klein, J. Math. Phys. **64**, 1735 (1977).
[29] W. Klein and N. Grewe, J. Chem. Phys. **72**, 5456 (1980).
[30] W. Klein and A. C. Brown, J. Chem. Phys. **74**, 6960 (1981).
[31] W. Klein, H. Gould, R. A. Ramos, I. Clejan, and A. I. Mel'cuk, Physica A **205**, 738 (1994).
[32] F. H. Stillinger and D. K. Stillinger, Physica A **244**, 358 (1997).
[33] J.-P. Hansen and L. Verlet, Phys. Rev. **184**, 151 (1969).
[34] J.-P. Hansen and D. Schiff, Mol. Phys. **25**, 1281 (1973).
[35] M. Watzlawek, H. Löwen, and C. N. Likos, J. Phys.: Condens. Matter **10**, 8189 (1998).
[36] H. L. Frisch, N. Rivier, and D. Wyler, Phys. Rev. Lett. **54**, 2061 (1985).
[37] W. Klein and H. L. Frisch, J. Chem. Phys. **84**, 968 (1986).
[38] H. L. Frisch and J. K. Percus, Phys. Rev. A **35**, 4696 (1987).
[39] B. Bagchi and S. A. Rice, J. Chem. Phys. **88**, 1177 (1988).
[40] The small discrepancies between MFA and MC for $g(r)$ at small r values disappear as the density is increased. Perfect agreement between theory and simulation can be achieved if, instead of the MFA, one employs the HNC or some more refined version of the MFA to calculate the fluid structure, see Refs. [22] and [26].